

Supplement to
AMMRC MS 82-4

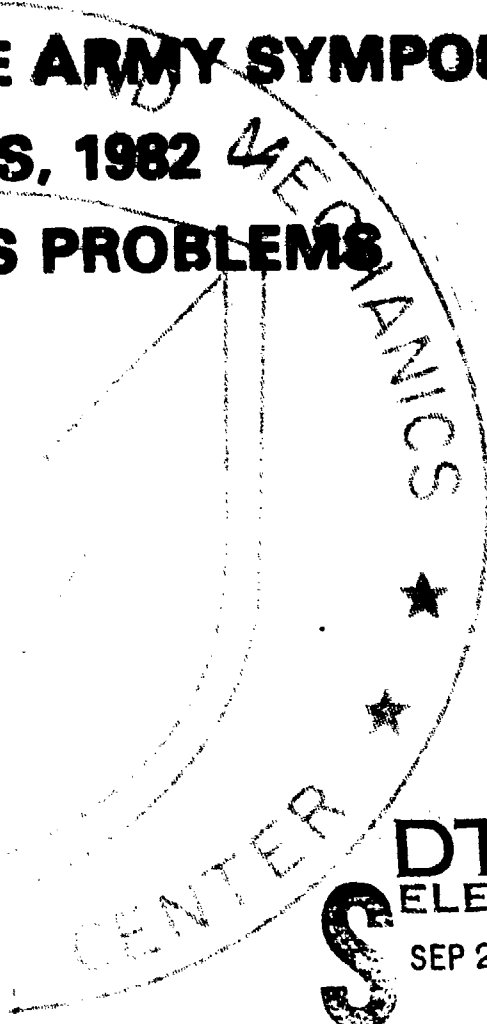
AD

①②

AD A119498

**SUPPLEMENT TO THE
PROCEEDINGS OF THE ARMY SYMPOSIUM
ON SOLID MECHANICS, 1982
CRITICAL MECHANICS PROBLEMS
IN SYSTEMS DESIGN**

September 1982



DTIC
ELECTE
SEP 23 1982

A

DTIC FILE COPY

Approved for public release; distribution unlimited.

ARMY MATERIALS AND MECHANICS RESEARCH CENTER
Watertown, Massachusetts 02172

82 09 23 001

The findings in this report are not to be construed as an official Department of the Army position, unless so designated by other authorized documents.

Mention of any trade names or manufacturers in this report shall not be construed as advertising nor as an official endorsement or approval of such products or companies by the United States Government.

DISPOSITION INSTRUCTIONS

Destroy this report when it is no longer needed.
Do not return it to the originator.

PREFACE

This document contains a paper that was intended to be included with-
in the proceedings of the Army Symposium on Solid Mechanics, 1982 on pages
43-65, but was not because approval to do so was not obtained from higher
authorities in time for such incorporation. The proceedings are contained
within Army Materials and Mechanics Research Center, Manuscript Series
Report, AMMRC MS 82-4, dated September 1982.

AMMRC Form 100
CLASSIFICATION
DATE
BY

A



BLAST RESPONSE OF A HARDENED ARMY ISO SHELTER

Roger W. Milligan, Kaman AvIDyne
Allen Lush, Kaman AvIDyne
William L. Crenshaw, U.S. Army Natick
Research and Development Laboratories

ABSTRACT

The U.S. Army at Natick (NLABS) is presently conducting a program to develop a nuclear hardened, mobile, tactical shelter which would be used to house C³ systems. As part of this program, a prototype shelter was designed to withstand a blast loading corresponding to a 10.0 psi (68.9-kPa) incident overpressure. The hardened shelter was then constructed, instrumented and subjected to a simulated nuclear blast loading at the MILL RACE test, White Sands Missile Range, New Mexico. The principal objectives of the test were to evaluate analytical methods for predicting shelter structural effects and shelter overturning effects induced by blast loading and to assess the validity of a particular design concept using conventional materials. Comparison of measured versus predicted values of shelter wall strain and shelter overturning motion confirm the validity of the analytical methods used. Test results demonstrated that a design featuring shear stiffened sandwich panels with aluminum face materials could withstand a nominal 10.0 psi incident shock loading.

INTRODUCTION

The U.S. Army has a requirement for the development of nuclear hardened shelters which will be used to house command, control and communications (C³) systems. In response to this requirement, the U.S. Army Labs at Natick (NLABS) has funded a research and development program directed to the development of an optimized (minimum weight and cost) nuclear hardened shelter. One phase of this program, reported herein, involved an evaluation of analytical methods for hardened shelter design and the structural evaluation of a particular design concept using conventional materials of construction. The evaluation was performed by designing a shelter featuring shear-stiffened sandwich panels with aluminum face materials to withstand a 10.0 psi (68.9-kPa) incident overpressure, subjecting the shelter to a simulated nuclear blast loading, measuring shelter response, and comparing the measured results with calculated values. The hardened shelter experiment was conducted at the MILL RACE Test, White Sands Missile Range, New Mexico.

A tactical shelter in the vicinity of a nuclear detonation would be subjected to an intense thermal pulse followed by a shock wave-induced blast loading. The thermal pulse could induce high temperature and thermal stress in the shelter wall. Blast loading phenomena are associated with combined overpressure loading and drag loading which is induced by the material velocity behind the shock wave. During early times after shock arrival, the effects of overpressure predominate, and

it is during this phase (diffraction phase) that the maximum deformation of the shelter walls occurs. At latter time, the effects of drag loading predominate, and the shelter is subjected to overturning motions.

For this program, only the effects of blast loading on the shelter were evaluated. The shelter experiment did not simulate a thermal pulse. The blast loading was simulated by the detonation of 600 tons (5.33 MN) of ANFO and was equivalent to a 1 KT (8.89 MN) ground burst.

SHELTER CONFIGURATION

Details of the prototype shelter design configuration are shown in Figure 1. As indicated, the shelter is a six sided box structure approximately twenty feet (6.1m) long by eight feet (2.44m) high and eight feet (2.44m) wide. The shelter panels are identified as follows: windward side wall, leeward side wall, fore and aft end walls, roof and floor. Panel horizontal edges are joined by splice plates on the outside surfaces and splice angles on the inside surfaces (see Section AA). In a similar manner, panel vertical edges were joined to steel corner posts. Doors are provided in both end walls for access to the inside of the shelter. An aluminum base frame is attached to the floor and provides hard point structure for handling the shelter via fork lift or mobilizers. The eight corners of the shelter feature steel corner fittings which facilitate handling via sling, mounting on jacks or utilization as a shipping container. The shelter outside dimensions and corner fitting details conform to ISO/ANSI requirements. Thus the shelter is compatible with commercial truck, rail, sea carriers or container ship transportation modes.

Cross sectional details of the panels are shown in Section BB of Figure 1. As indicated, the walls were constructed of sandwich design and featured aluminum (6061-T6) face sheets with an 8 pcf (1.26 kN/m³) Nomex (aramid fiber/phenolic resin) core reinforced by an aluminum (6061-T6 extrusion) box shaped stiffener at 14.0 in. (.356m) spacing. Side wall faces and core are 0.16 in. (4.06mm) thick and 4.0 in. (.102m) thick, respectively. Corresponding dimensions for the roof are 0.10 in. (2.54mm) and 3.0 (.076m) inches. Cross sectional details for the roof and floor are identical. The cross sectional details for the end walls are the same as the side walls except that the core is not reinforced by stiffeners. For a detailed description of the design approach and supporting analysis, see [1].

INSTRUMENTATION

The test instrumentation arrangement is illustrated in Figure 2. From Figure 2a, panel load distribution was measured by pressure gages mounted on the windward side wall and roof (eight gages total). The windward side wall gages were located to measure vertical and longitudinal pressure distribution near or at the panel centerline

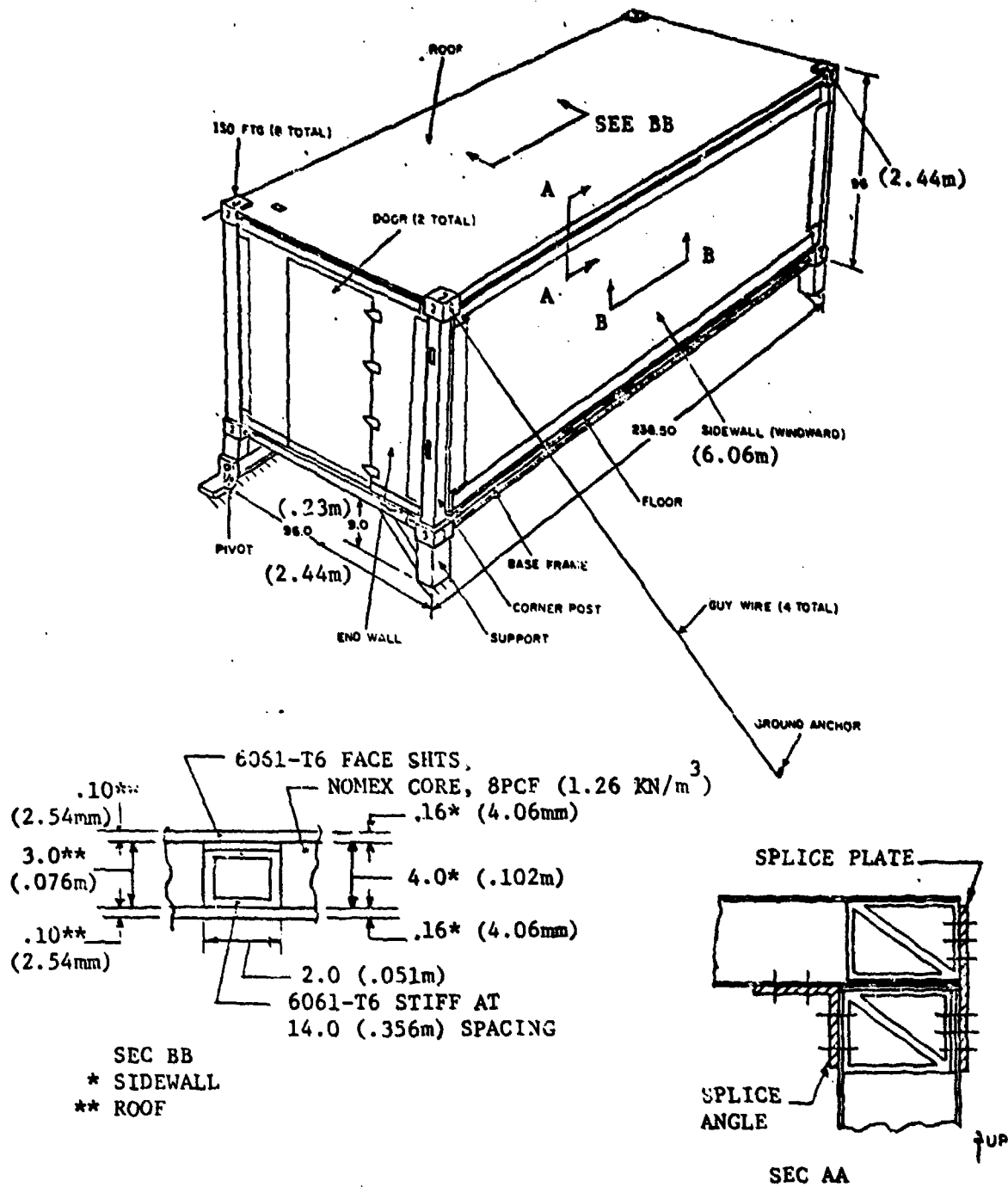
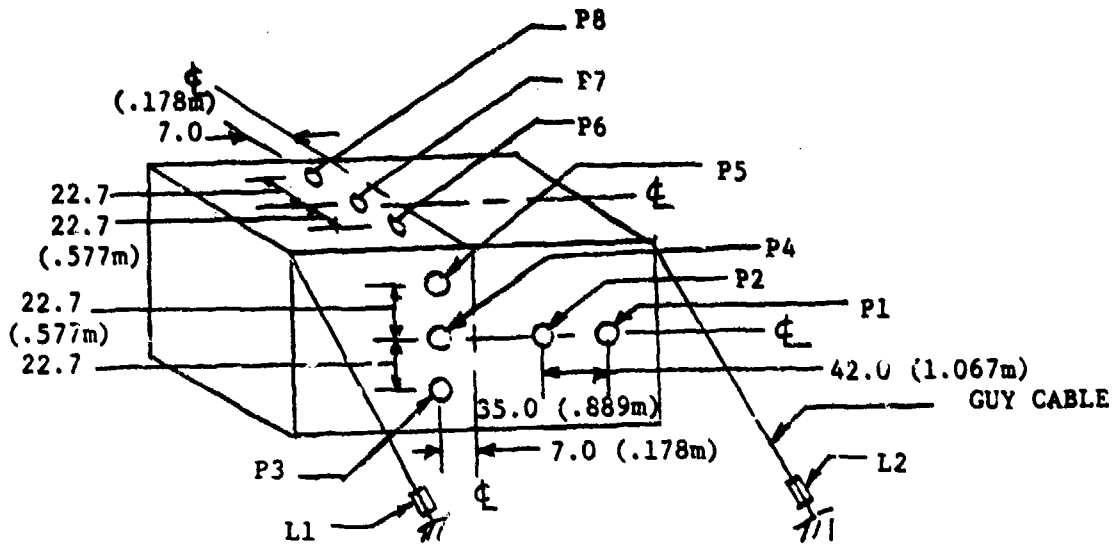
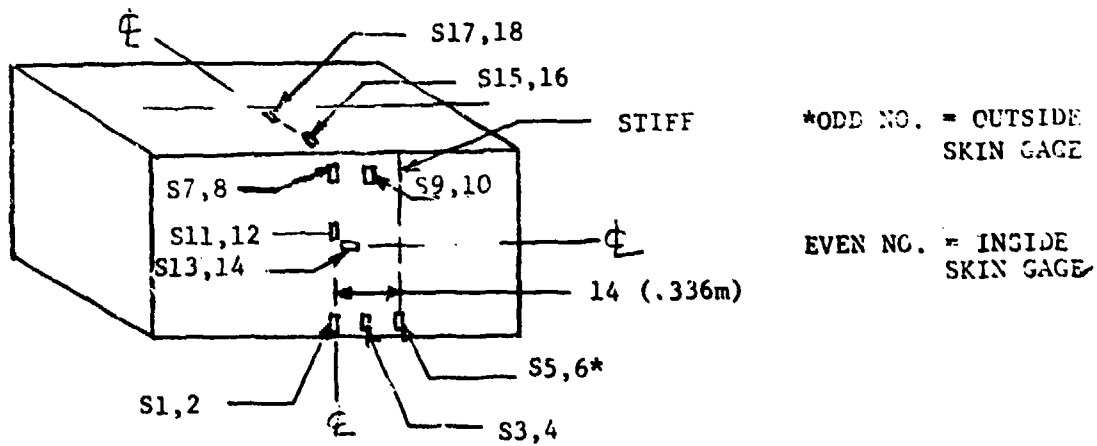


Figure 1. Shelter Configuration



a) Pressure (P) Gages and Load (L) Cells



b) Strain (S) Gages

Figure 2. Shelter Instrumentation

locations. The roof gages were positioned to measure lateral load distribution near the roof centerline location. On the windward side of the shelter, load cells were installed in series with the guy cables near the ground anchor terminations to measure guy wire load.

Shelter panel strain was measured using the strain gage instrumentation arrangement of Figure 2b. Strain measurements were made at twelve locations on the windward side wall and four locations on the roof. Gages were positioned to measure vertical centerline side wall strain at the panel center (S11, 12; S13, 14), bottom edge (S1,2) and top edge (S7,8). In addition, strain was measured between stiffeners (S3,4; S9,10) and at a second stiffener location (S5,6). As indicated, the gages were mounted on the outside (odd numbered gages) and inside (even numbered gages) faces of the sandwich panel. All gages were EA-13-12SBT-120 uniaxial strain manufactured by Micro-Measurements.

In addition to instrumentation shown in Figure 2, three high speed cameras were used to photograph shelter behavior. Of particular importance was a camera located outside the shelter to photograph overturning motions. A second outside camera was located in front of the shelter to photograph motions of the windward side wall. A third camera inside the shelter was positioned to record motions of the inner surface of the windward side wall. External cameras were housed in a protective box mounted on a rigid pedestal. As an aid in the interpretation of high speed photographs of shelter motions, vertical reference poles were located outside the shelter near the four shelter corners.

TEST ARRANGEMENT

Details of the shelter test arrangement are illustrated by the schematic in Figure 1. As indicated, the shelter was mounted on four vertical struts located at each lower corner such that the floor of the shelter was approximately nine inches (.23m) above the ground. This arrangement simulated a shelter installed on the ground with jacks. In order to provide support constraints that could be exactly modeled during computer simulation, the supports were designed such that forward struts could lift off the ground. The rear struts were pinned to a base fitting fixed to the ground such that the shelter could rotate in roll about the rear pivot (see Figure 1). To restrain shelter overturning motions, tie down cables were connected from each of the upper corners of the shelter to ground anchors. The 9/16 in. (14.3mm) diameter cables were fabricated from Nomex material. Static tests of the Nomex cable indicated a much greater energy absorbing capacity than conventional steel cables. The Nomex cable design was developed by the HATS program [2].

For the test, the shelter was positioned approximately 980 feet (300 m) from ground zero and oriented such that the windward side wall was parallel to the plane of the incident shock wave. A 10,000 lb (44.5 kN) payload was simulated with sand bags placed on the floor of the shelter.

POST TEST EXAMINATION OF THE SHELTER SYSTEM

After the MILL RACE test an inspection of the shelter and support structure revealed the following:

- The shelter structure survived the test blast loading without any apparent failure or permanent deformation.
- Based on a "tapping evaluation" of the shelter walls in anticipated high stress areas, there was no apparent delamination of the sandwich skin, core or stiffener components.
- Structural failures occurred in the shelter support system. Both windward side guy wires failed at the joint between the Nomex cable and termination fitting. Some of the fasteners used in the base support system failed in shear.
- The overturning motions of the shelter were apparently small since all interior equipment such as sand bags and camera tripods remained in place following the test. This was verified by high speed motion pictures and analysis.

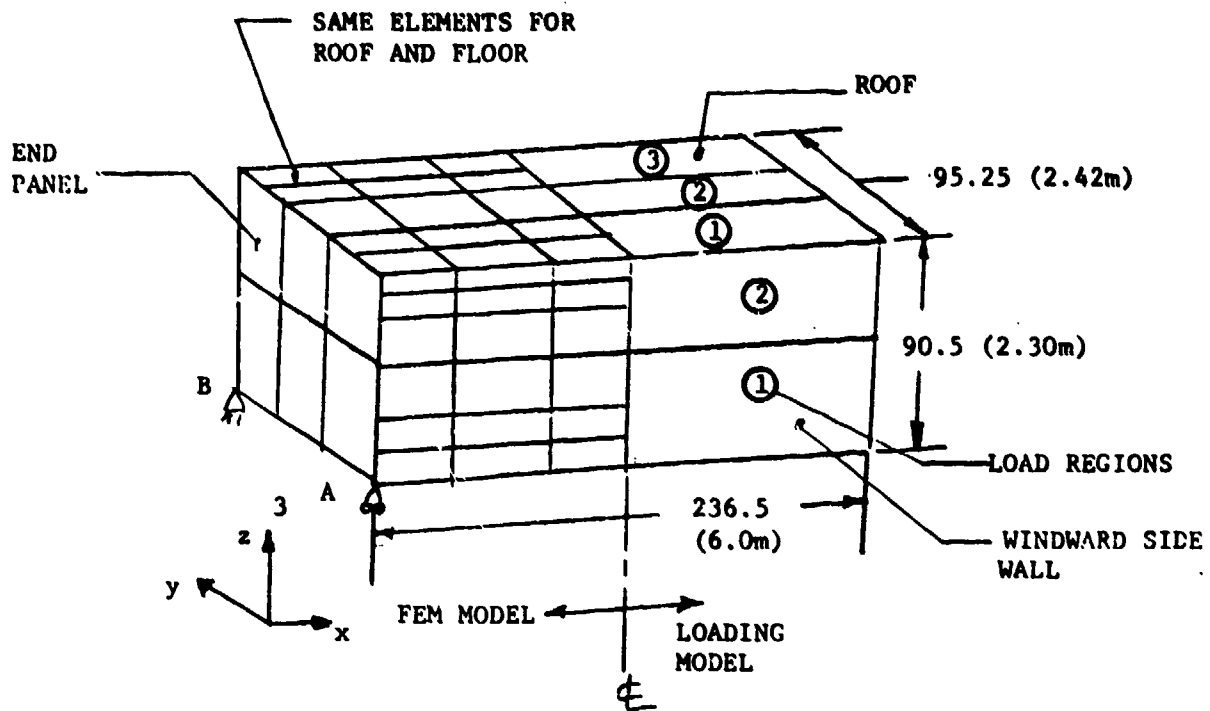
SHELTER STRUCTURAL RESPONSE

ANALYSIS METHODS

A finite element model was made of the shelter structure, and the theoretical shelter structural response was determined using the ADINA finite element computer code [3]. The walls of the shelter were modeled using an "equivalent layer" representation of the sandwich components (face material, core and internal stiffeners). A procedure for calculating equivalent layer properties for use with ADINA's 3-D solid element was developed by Kaman AviDyne [4]. Use of this approach allowed a significant reduction in model degrees of freedom.

Shelter modeling and pressure loading details are summarized in Figure 3. Due to symmetry, it was only necessary to model one half the shelter. Since the principal region of interest for shelter response was the windward side panel and roof, these panels were modeled with a finer mesh of elements than the end wall or leeward side wall. Eighteen elements were used to model the windward side wall, and fifteen elements were used for the roof and floor. Only six elements were used for the end and leeward side walls. The model also included elements at the panel edges to represent shelter edge members, corner fittings and post structure. A total of 82 elements was used in the model.

As shown in Figure 3, the shelter model was restrained at the four bottom corners. At the aft support points, both the vertical (δz) and lateral (δy) deflections were restrained. Only the vertical deflection (δz) was restrained at the forward support points. It was not considered necessary to include the guy wires in the model. The loads developed by the guy wire during the time of peak panel response are



SUPPORT PT. B, $\delta_x = \delta_y = 0$

SUPPORT PT. A, $\delta_z = 0$

Figure 3. Finite Element Model (FEM) and Pressure Loading Model for Shelter Analysis

relatively small (1500 lbs/wire) (6.68 kN/wire), and have a negligible effect on the strain at the panel center due to the large distances involved.

Details of the pressure loading regions are illustrated in the right side of the shelter schematic (Figure 3). As indicated, the windward side panel was divided into two loadings regions. For the roof and floor panels, three pressure loading regions were used in order to represent the effect of the pressure wave moving across the surface. Although not shown in the figure, a single pressure-time history was used for the end wall and the leeward side wall.

For the theoretical analysis of the shelter response, the pressure-time history used for each of the regions shown in the schematic was based on pressure gage measurements from the MILL RACE test. For the side wall, panel loading for Regions 1 and 2 was based on P3 and P5 pressure data, respectively (see Figure 2). Roof and floor panel loading for Regions 1, 2 and 3 were based on P6, P7 and P8 pressure data, respectively. For the end panels and leeward side panel, no pressure test data were available. In this case, the pressure loading used was based on theoretical results for a point at the panel center obtained by use of the BLOCK code [5].

For the MILL RACE test, the actual measured shelter incident overpressure loading was 9.0 psi (62.0 kPa) [6]. Characteristics of the pressure loading on the windward side wall and roof are illustrated by the measured pressure loading curves of Figure 4. For the windward side wall, at shock arrival time (365 msec), Gage P5 results show a nearly instantaneous increase in overpressure to a value of 23.5 psi (161.9 kPa) followed by an exponential decrease with time. The peak side wall overpressure of approximately 2.6 times the incident overpressure is caused by shock wave reflection [7]. For the roof gage closest to the windward side wall (P6), the pressure/time history is characterized by a maximum value of 9.0 psi (62.0 kPa) at shock interception followed by an exponential decay. The large perturbation in the measured pressure curve centered at 380 msec is attributed to the formation of vortex flow at the windward side wall/roof corner which propagates along the roof and diffuses as it approaches the leeward side wall [8].

COMPARISON OF RESULTS

Comparison between calculated (dashed line) and measured strain (solid line) for the windward side wall is shown in Figures 5, 6 and 7. The figures correspond to strain gage locations at the panel center, near the panel floor edge and near the panel roof edge, respectively. For each location, results are given for both the outside and inside face strain gage locations. The strain response in all cases is characterized by two strain peaks which occur approximately six and

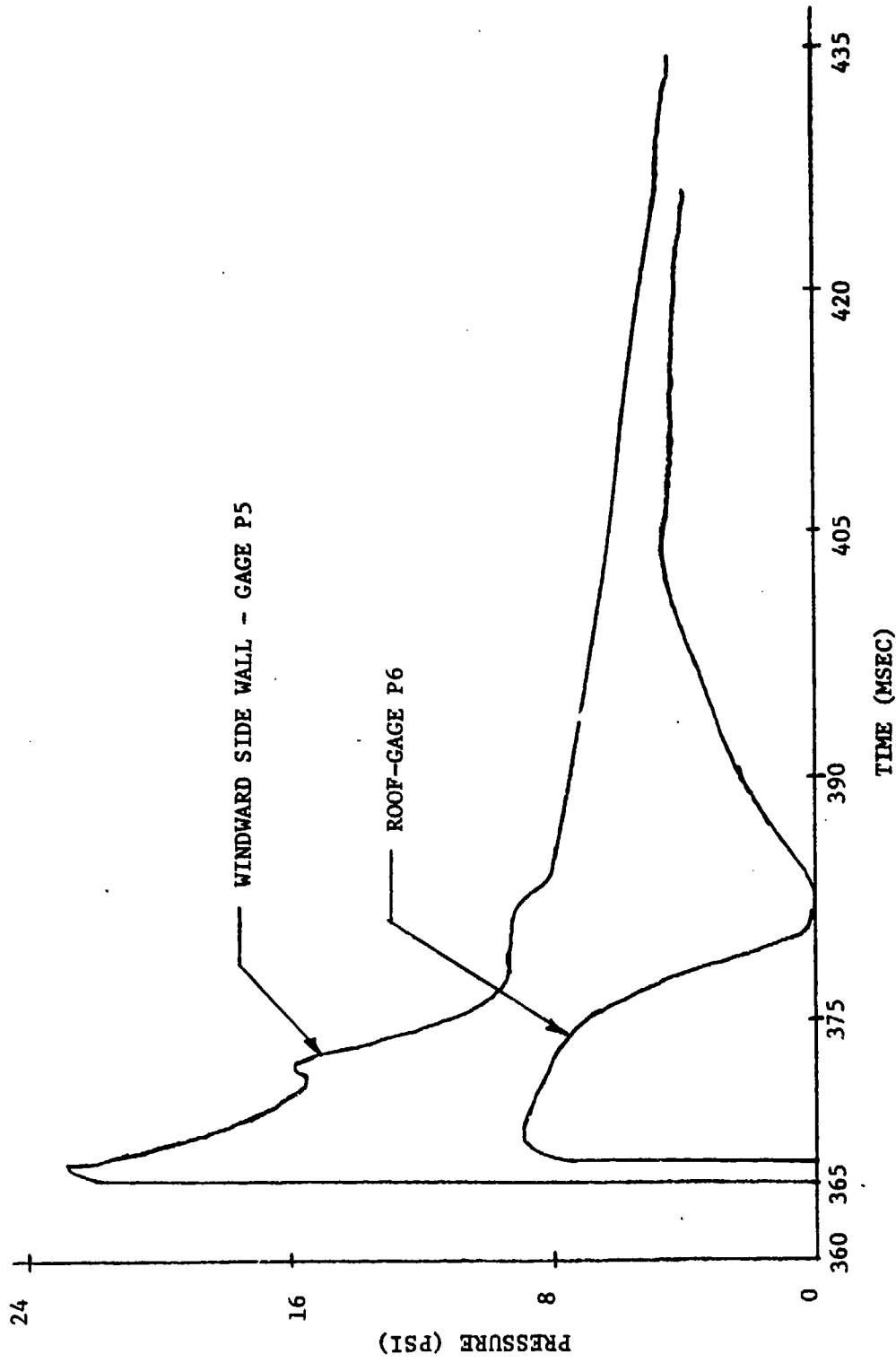
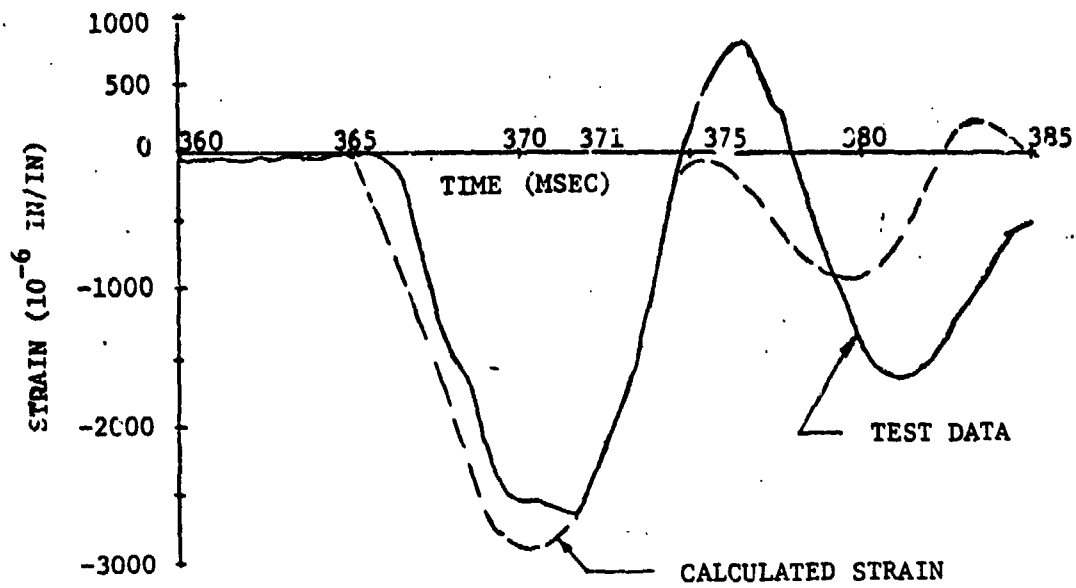
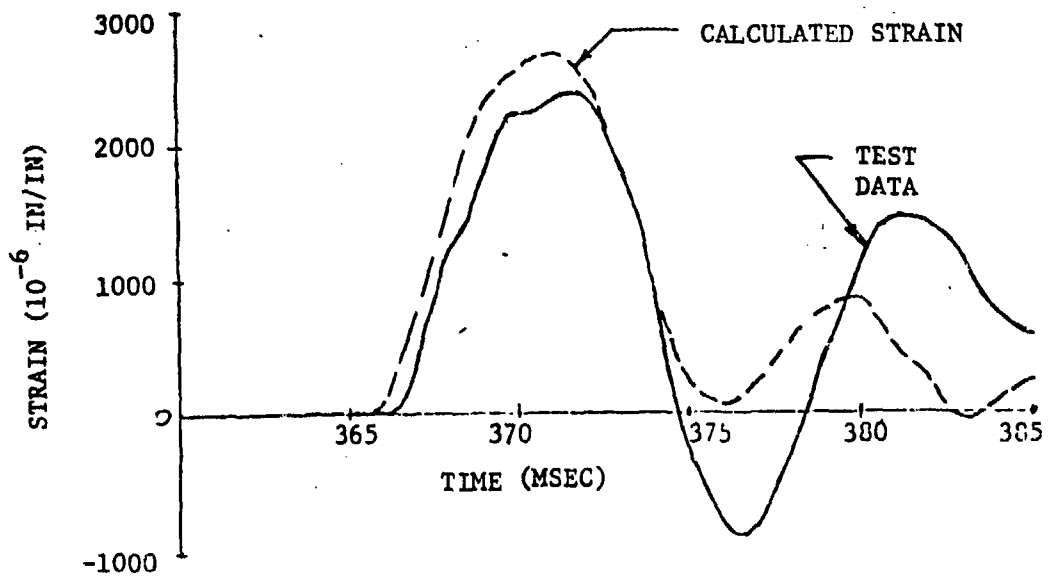


Figure 4. Pressure Loading Characteristics for Windward Side Wall and Roof

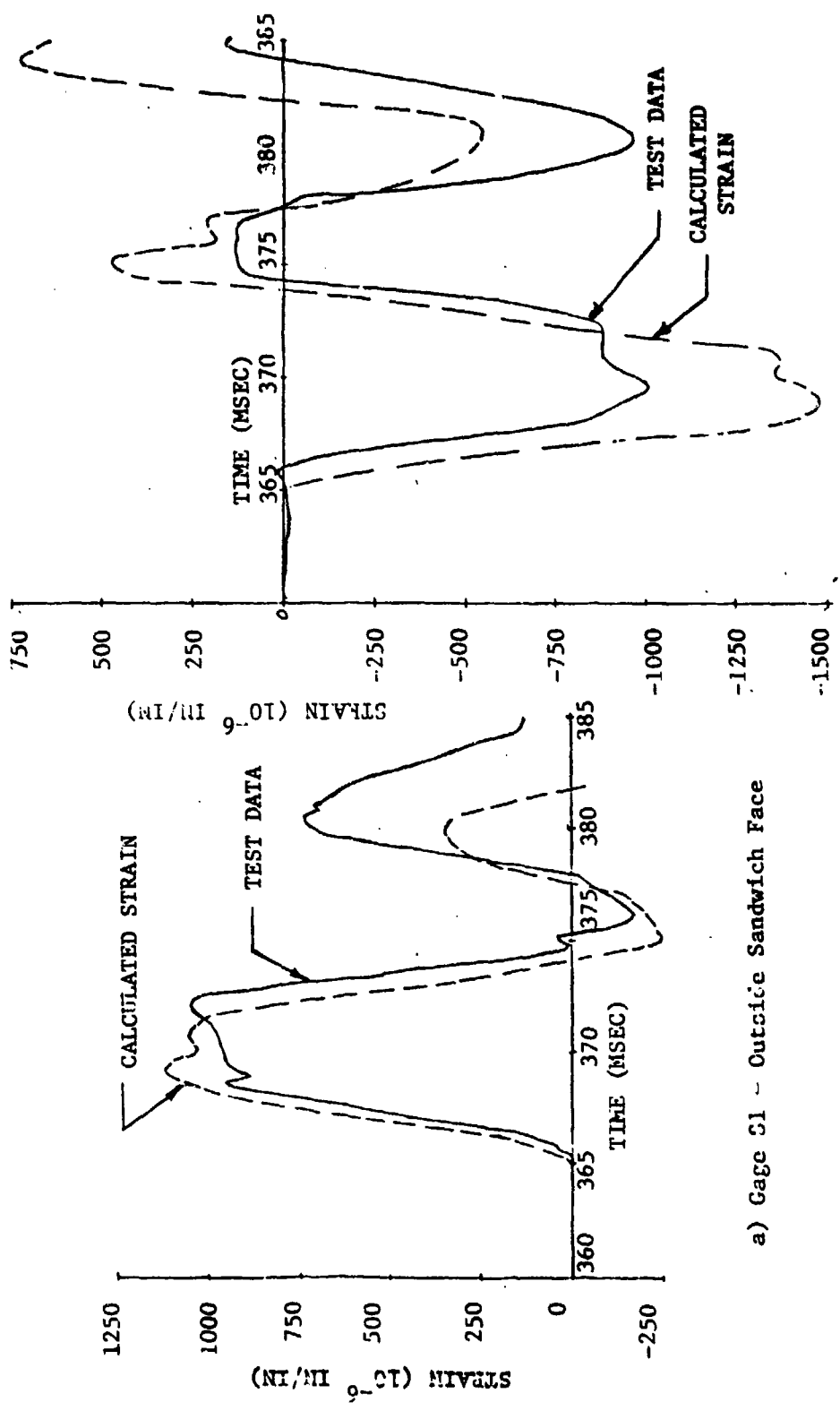


a) Gage S11 - Outside Sandwich Face



b) Gage S12 - Inside Sandwich Face

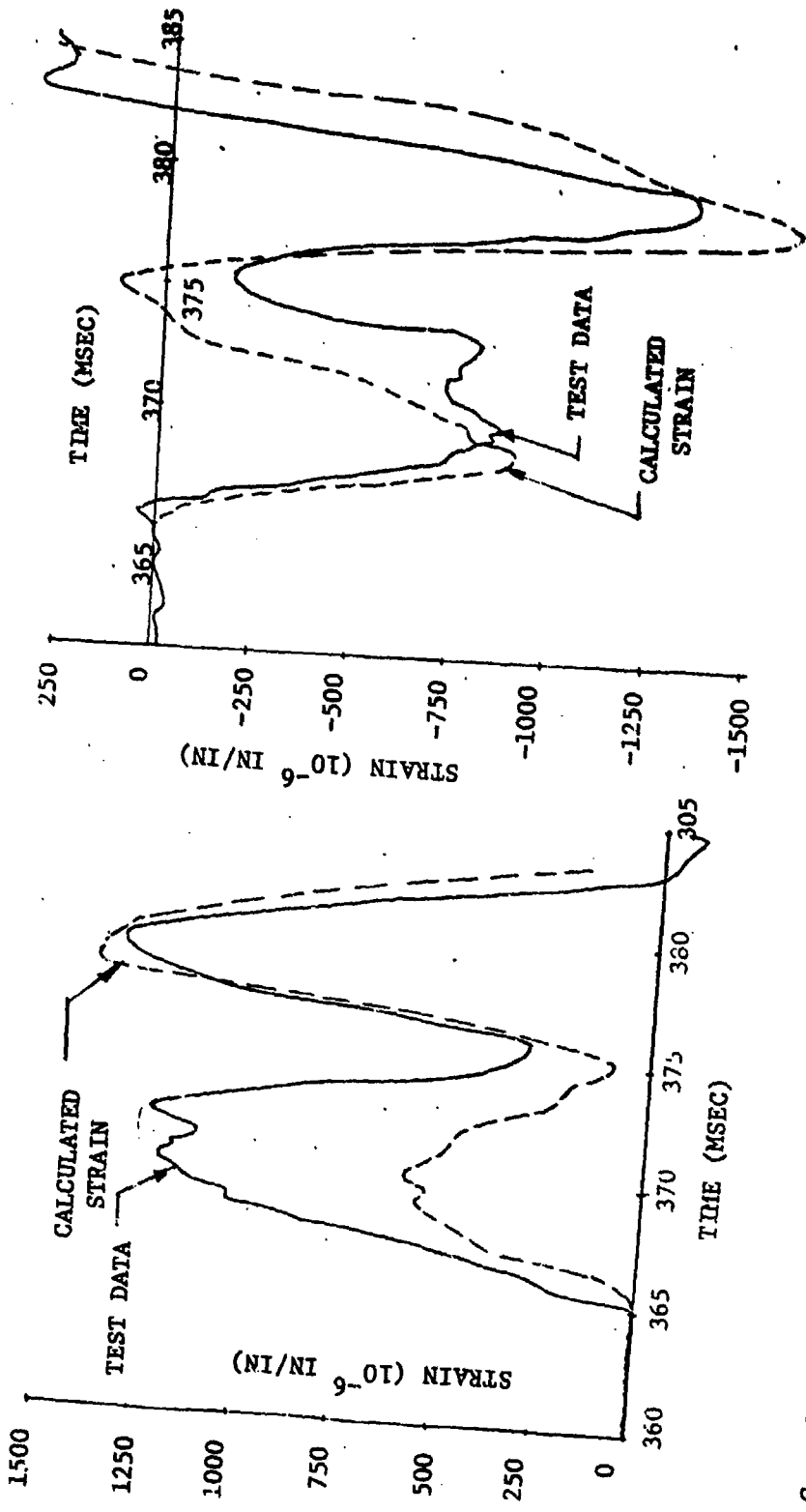
Figure 5. Windward Side Wall Strain at the Panel Center



b) Cage S2 - Inside Sandwich Face

a) Cage C1 - Outside Sandwich Face

Figure 6. Windward Side Wall Strain near the Floor



a) Gage S7 - Outside Sandwich Face

b) Gage S8 - Inside Sandwich Face

Figure 7. Windward Side Wall Strain near the Roof

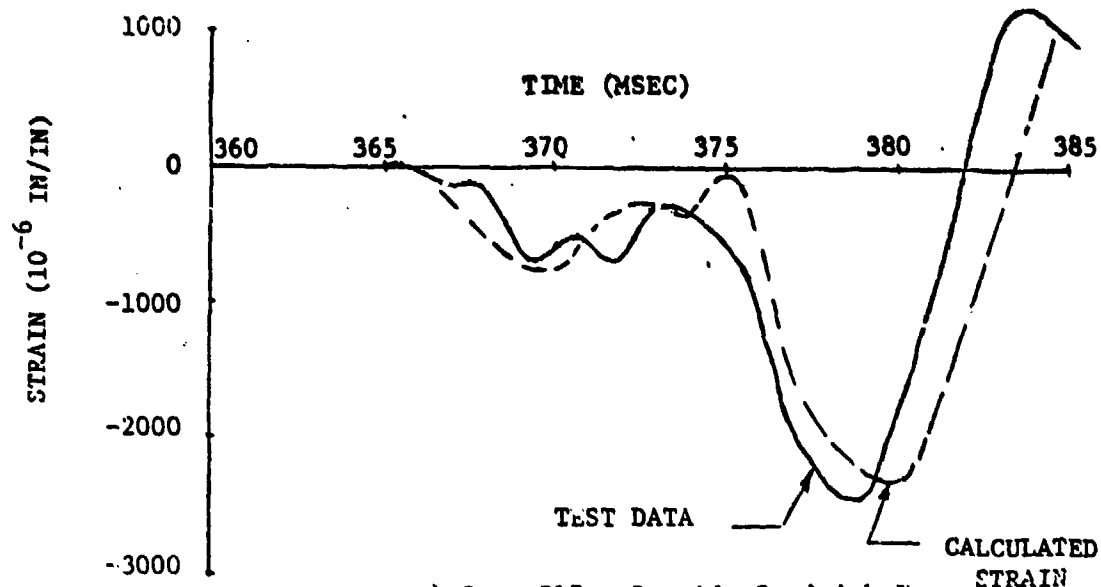
seventeen milliseconds after shock arrival. Hence, peak panel response occurs shortly after shock arrival. All calculated response curves were based on an equivalent blast yield of 0.6 KT (5.33 kN).

Figure 5 shows excellent agreement between calculated and measured strain corresponding to the first and largest strain peak at the center of the windward side wall. For the smaller strain peak, the calculated response is less than that shown by the measured data. In Figure 6, showing strains near the panel floor, the first calculated strain peak is in excellent agreement with the measured data for the outside gage (S1) but overestimates the strain at the inside gage location (S2). For the second strain peak, one observes that the maximum calculated strain is less than the measured value at both gage locations. As shown in Figure 7, near the roof there is excellent agreement between calculated and measured strain values for the first peak of the inside gage (S8); however, for the outside gage (S7), the calculated peak response is much less than the measured value. At this panel location, the curves of Figure 7 show that the maximum strain value for both gages corresponds to the second strain peak. As this critical response time (approximately 380 msec), there is good agreement between calculated and measured strain for both gages. For all the windward side panel strain plots shown, the frequency characteristics of the calculated response follow the measured data.

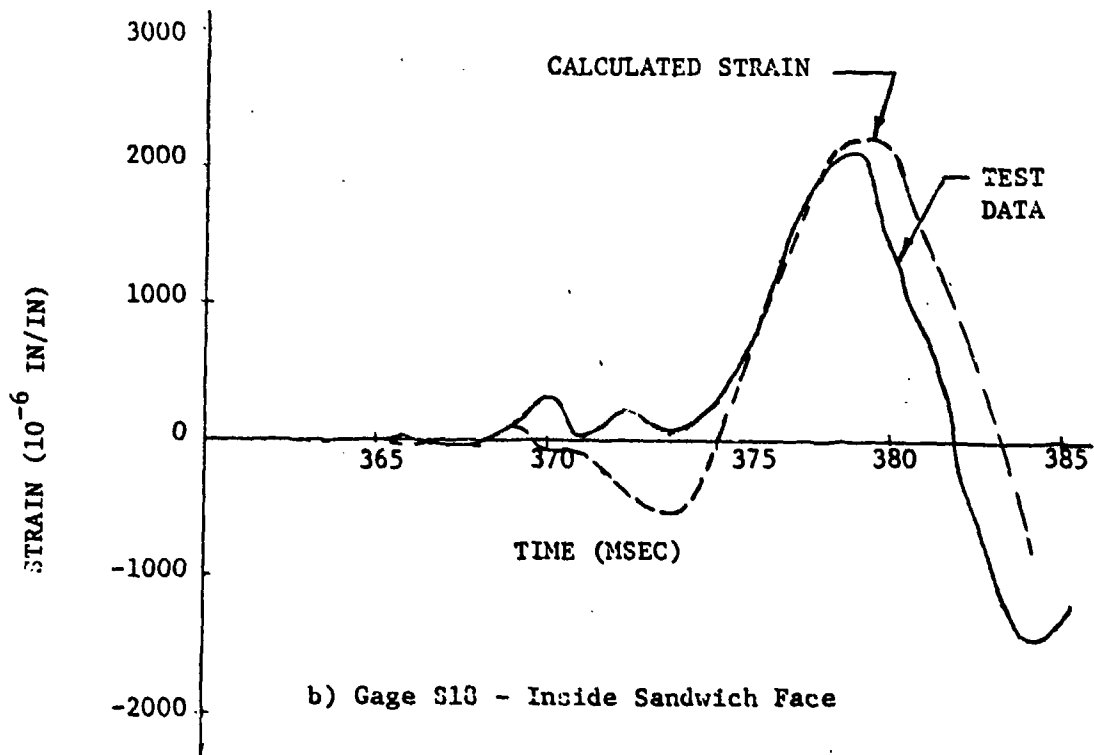
One observes from the peak measured strains shown in Figures 5, 6, and 7 that maximum strain occurred at the panel center (-2600 μst , Figure 5a) and was significantly larger than corresponding values near the floor (+1040 μst , Figure 6a) or near the roof (+1340 μst , Figure 7a). For a vertical width of wall along the panel center, one would expect the behavior to be similar to that of a beam. It is noted that for a beam with clamped edges, the strain at the ends would be twice that at the panel center [9]. The beam analogy suggests that the windward side wall edge fixity is considerably less than that corresponding to a clamped condition.

Comparison between calculated and measured strain at locations near the center and windward side wall edge of the roof are shown in Figures 8 and 9. At both locations, strain response is shown for both the outside and inside gage locations. One observes that the roof strain response is also characterized by two strain peaks which occur at essentially the same time as the windward side wall. However, the relative magnitude of the first strain peak is drastically reduced at the roof center as compared with the roof edge.

At the roof center, the strain curves of Figure 8 show excellent agreement between calculated and measured strain for both the outside (S17) and inside (S18) gages. At the roof edge location (Figure 9), the curves show good agreement between the calculated and measured values for the first strain peak. The second calculated peak strain is greater than the measured value. As before, the roof strain curves show

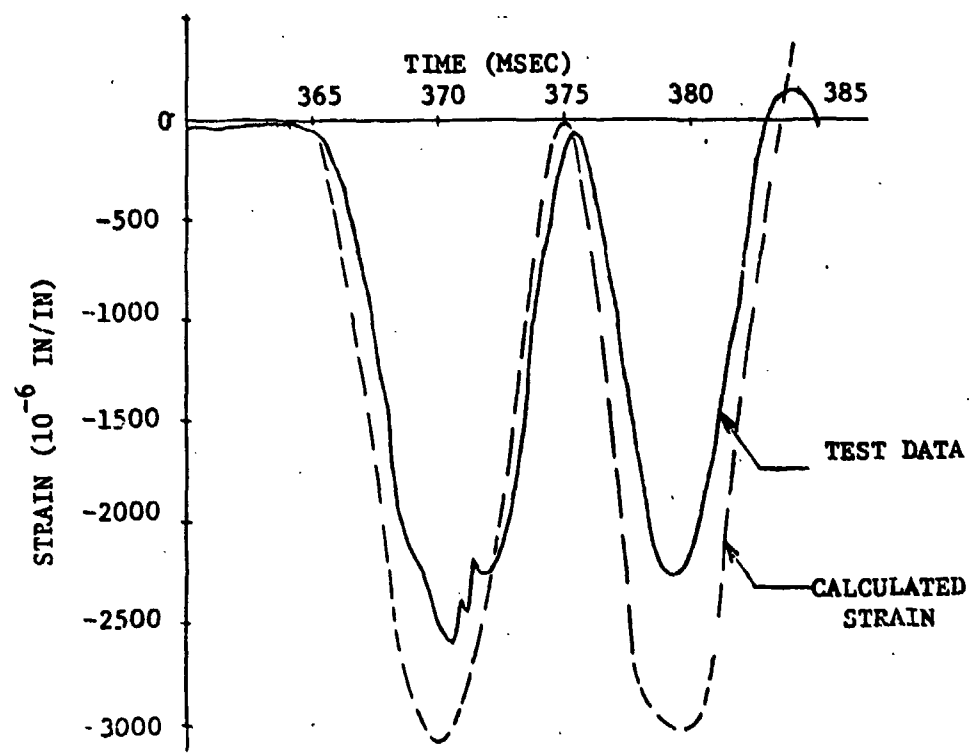
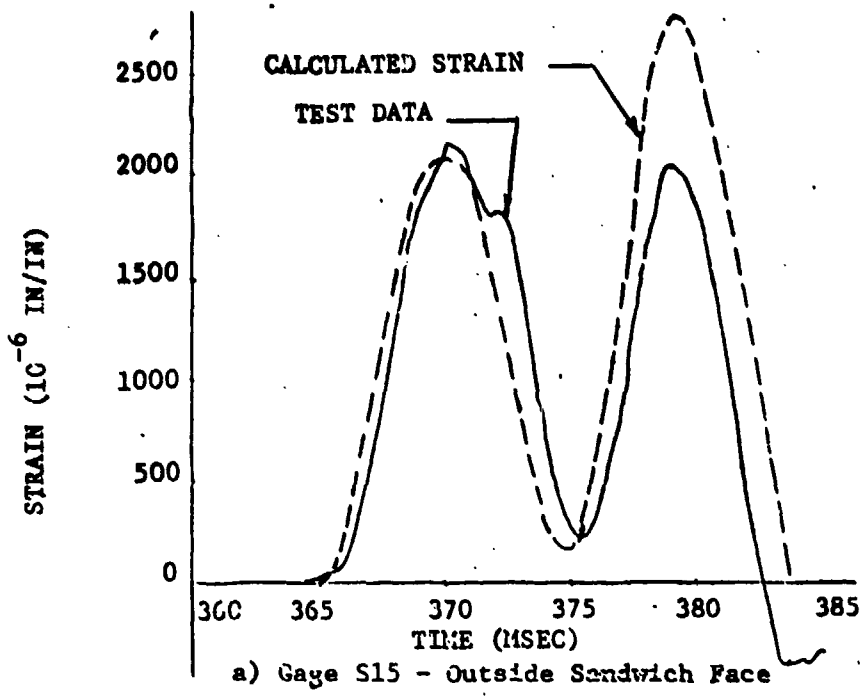


a) Gage S17 - Outside Sandwich Face



b) Gage S18 - Inside Sandwich Face

Figure 8. Roof Strain at the Panel Center



b) Gage S16 - Inside Sandwich Face
 Figure 9. Roof Strain near the Windward Side Wall

that the frequency characteristics of the calculated response follow the measured data.

Comparison between the maximum measured strain (second strain peak) for the roof center and edge locations on the outside face (S17 and 15) show that the maximum roof strain occurs at the panel center (2400 μ st vs -2000 μ st). The larger edge/center strain ratio for the roof panel as compared to the side wall indicates a larger edge fixity for the roof.

SHELTER OVERTURNING RESPONSE

As noted in the introduction, blast loading produced by a nuclear detonation can cause vehicle overturning. Hence, the design of a vehicle installation to survive a given blast loading level should include an assessment of the overturning threat.

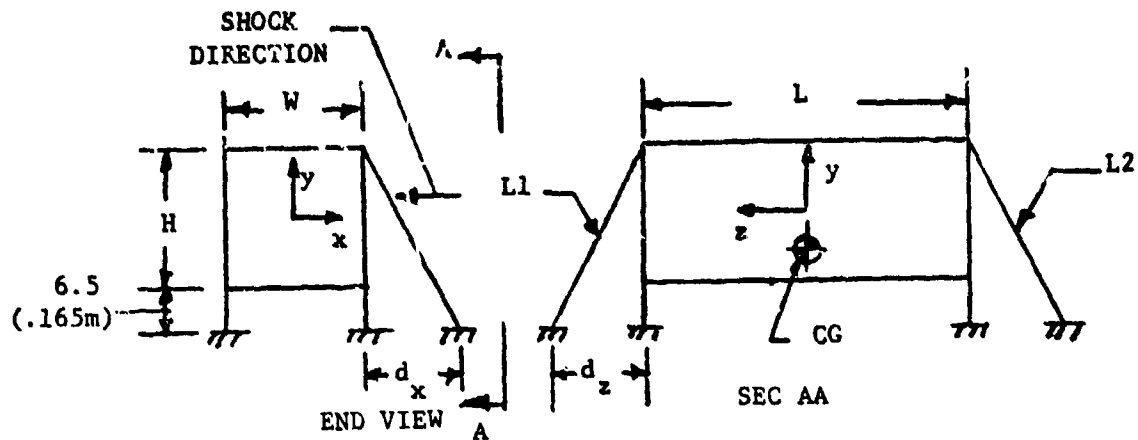
For the MILL RACE event, the shelter was exposed to a dynamic pressure pulse of relatively short duration (positive phase duration of approximately 0.20 seconds). As a result the aerodynamic forces on the shelter were not sufficient to cause vehicle overturning even without guy cable restraints. However, in order to evaluate options available in the overturning analysis, guy cables were attached between the four top corners of the shelter and anchor points on the ground. In order to provide controlled shelter boundary conditions, the leeward support struts were attached via a pivot joint to fittings anchored in the ground, and the windward support struts were free to lift off the ground (see Figure 1). With this arrangement, the shelter could not translate in the direction of the shock wave but was free to roll about the rear pivot.

ANALYSIS METHOD

The theoretical overturning response of the shelter to blast loading was determined using the TRUCK computer code developed by Kaman AviDyne [10]. The code can be used to determine the overturning response of vehicles incorporating a shelter system. In its most general form, the code accounts for oblique shock/vehicle intercept geometry, vehicle suspension system effects, nonlinear tie down restraints between the shelter and truck bed, and nonlinear guy cable restraints between the shelter and ground. The code includes a program for determining the aerodynamic forces on the vehicle/shelter combination. The output of the code includes a time history of the vehicle and shelter c.g. motions together with a parameter that indicates the degree of critical overturning.

For MILL RACE applications, the shelter was modeled as a rectangular shaped box on support struts. The TRUCK code was modified to allow pivoting of the shelter about the leeward support struts. Input parameters for the analysis are summarized in Table 1 and include

TABLE I. SHELTER CHARACTERISTICS FOR OVERTURNING ANALYSIS



Shelter Outside Dimensions

Length, $L = 236.5$ in (6.01m)
 Width, $W = 95.25$ in (2.42m)
 Height, $H = 95.0$ in (2.41m)

Shelter Weight and Mass Properties

$W = 18830$ lbs. (83.8 kN)
 $M = 48.8$ lb sec²/in (8550 kg)
 C.G. at $X = Z = 0$, $y_{cg} = -19.2$ in.
 $I_x = .303 \times 10^6$ lbs. in. sec.² (34.6×10^3 kg m²)
 $I_y = .305 \times 10^6$ lbs. in. sec.² (34.5×10^3 kg m²)
 $I_z = .0886 \times 10^6$ lbs. in. sec.² (10.03×10^3 kg m²)

Guy Cable Geometry and Preload (P)

for L1, $d_z = 32.0$ in (.813m), $d_x = 175.0$ in (4.47m), $P = 580$ lbs. (2.58 kN)
 for L2, $d_z = 26.0$ in (.650m), $d_x = 173.0$ in (4.39m), $P = 360$ lbs.
 (1.60 kN)

shelter outside dimensions, shelter weight and mass properties, and guy cable geometry and preload. The schematic in the table defines the shelter coordinate system and identifies shelter and guy wire parameters. The weight (W), mass (M) and mass moment of inertia (I) parameters correspond to a shelter weight of 8830 lbs (39.3 kN) and a simulated payload weight of 10,000 lbs (44.5 kN). Guy cable preload values shown were based on load test data.

Load-deflection characteristics of the guy cables required for the TRUCK code input were deduced from guy wire load cell test data and film of the shelter overturning motions. The roll angle of the shelter versus time was determined by advancing the film a known number of frames (film speed = 800 frames/sec) and measuring the angle between the shelter leeward side wall and a reference vertical pole. For a given roll angle, the guy cable strain was determined by the shelter and cable geometry. Corresponding to the time for a given roll angle, the associated guy cable load was determined from test data plots of guy cable load vs time.

Guy cable load-strain characteristics based on the above approach are presented as the dashed curves of Figure 10. Also shown in the figure are the Nomex cable lengths corresponding to the L1 and L2 installations. For the TRUCK input, guy cable load-deflection characteristics are input as load vs change in length. For a given force, the corresponding cable elongation for MILL RACE was determined by the product of cable length times percent elongation/100.

Also shown in Figure 10 is a static load deflection curve of the MILL RACE cable without termination fittings. One observes that compared with the static test results the MILL RACE cables evidenced a drastic reduction in strength and increased elongation for a given load. Since failure of both MILL RACE cables occurred at the termination fitting location, it is concluded that the details of the termination fitting/cable joint were responsible for the premature failure of the MILL RACE cables.

COMPARISON OF RESULTS

Based on the inputs described above and an equivalent blast yield of 0.6 KT (5.33 MN), overturning behavior of the MILL RACE shelter was determined via the TRUCK code. The calculated shelter roll angle versus time after shock arrival is shown in Figure 11 together with the shelter response based on test data. As previously described, the test results were based on measurements of shelter roll by viewing frames of the film recorded by the end view camera. The resulting test data is indicated by the circles in the figure, and the solid line represents a curve faired through the test data. As shown by the test curve, the maximum roll angle of the shelter was approximately 7° and occurred approximately 225 msec after shock arrival. Comparison of the calculated roll angle results with the faired test curve shows good agreement between theory and experiment. It is noted that the MILL

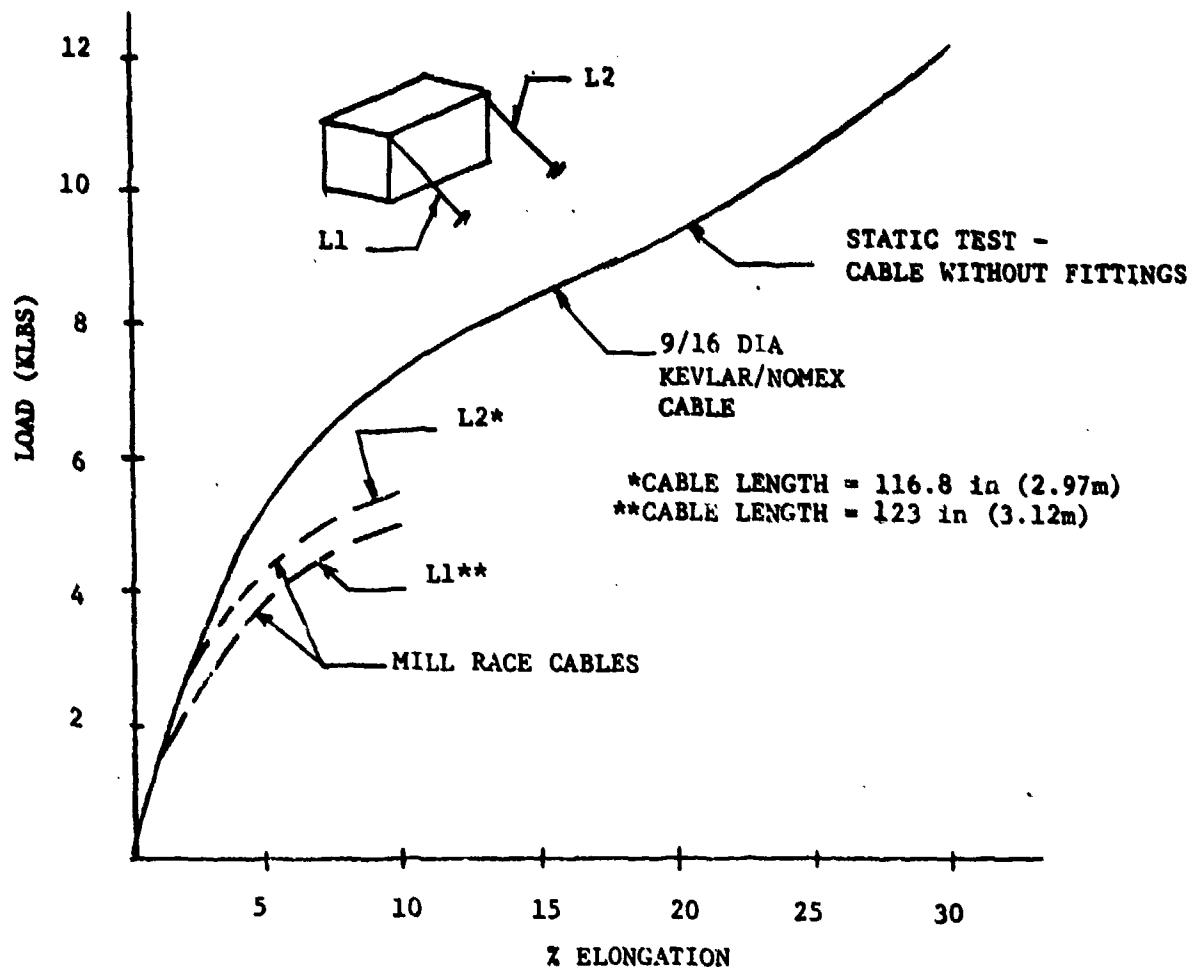


Figure 10. Load Versus Elongation Characteristics for MILL RACE Guy Cables

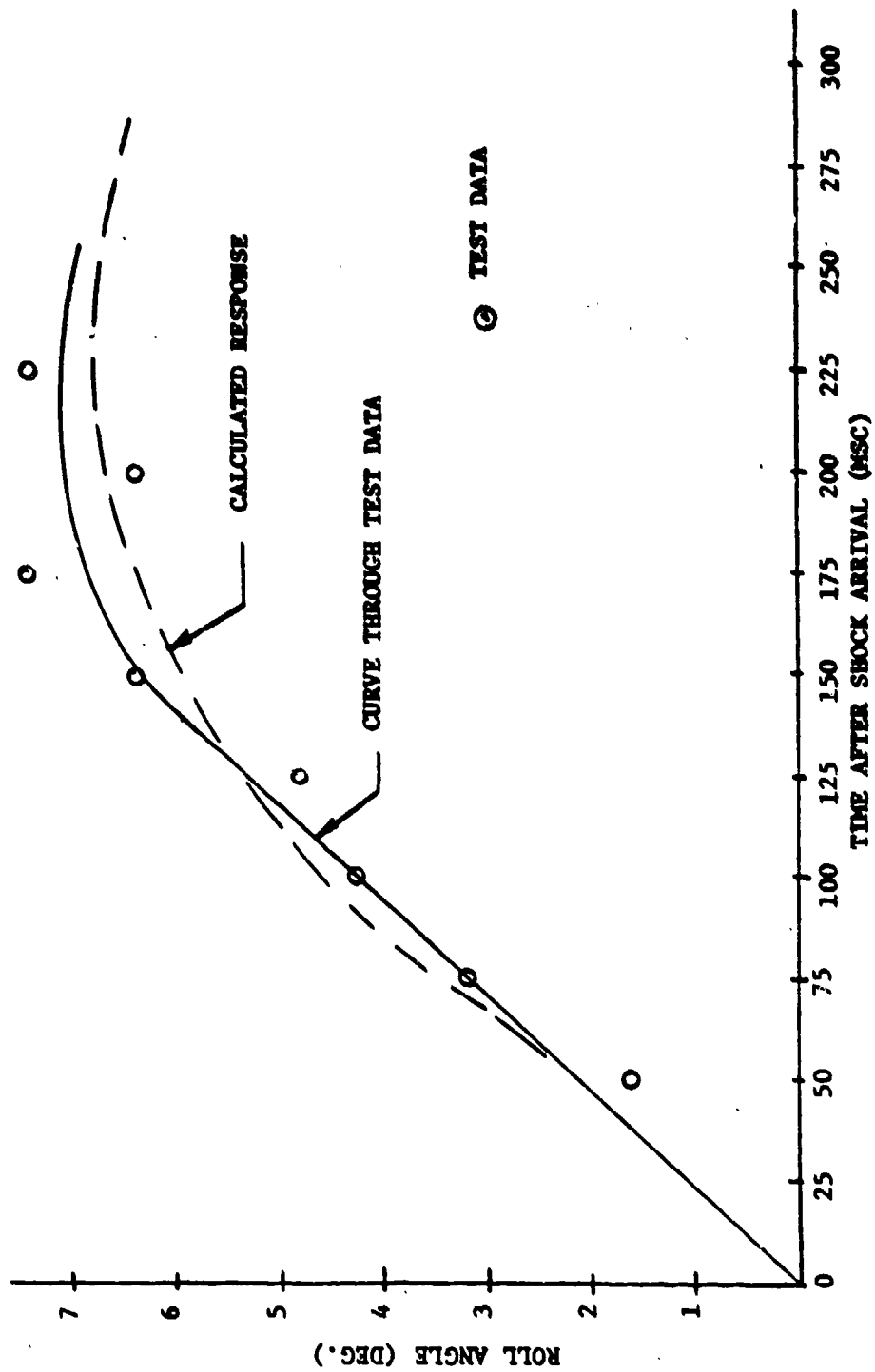


Figure 11. Shelter Overturning Response

RACE overturning analysis was repeated without guy cable restraints. For this case, the maximum roll angle was calculated to be 16.4°. Hence, the guy cables effectively reduced the maximum roll of the shelter even though they failed prematurely.

The theoretical guy cable response using TRUCK is shown in Figure 12 together with test data results. As shown by the figures, the calculated results are in good agreement with the test data.

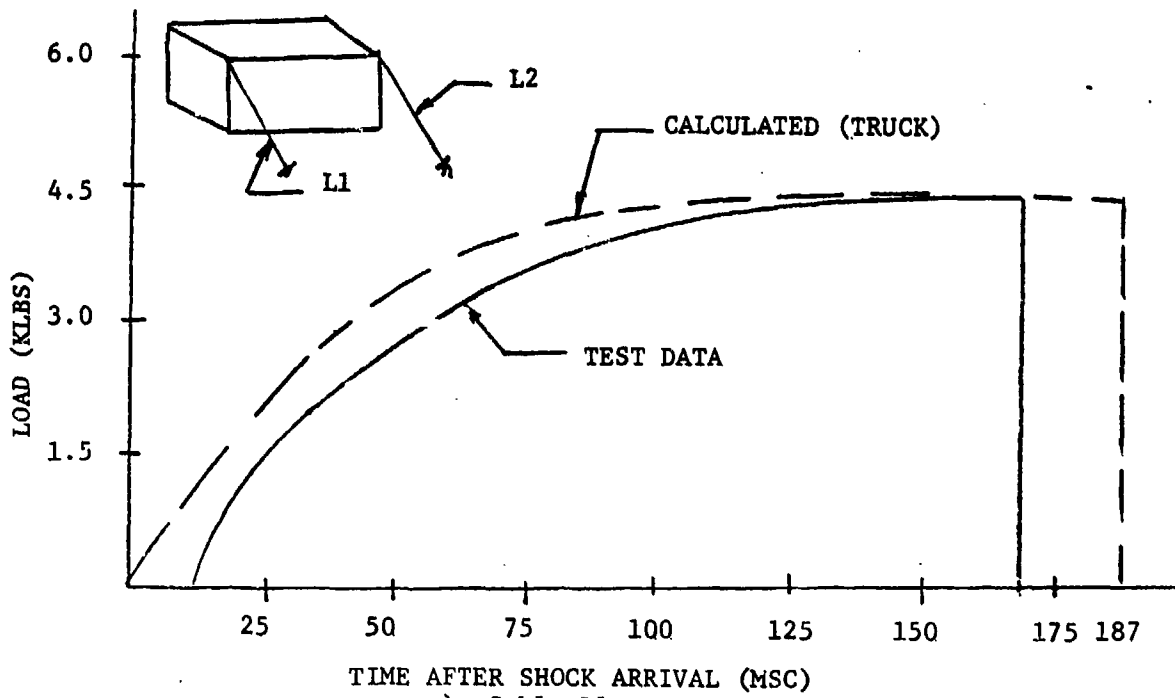
CONCLUSIONS

Based on an evaluation of test results and analysis methods used in the design of a shelter hardened for a nominal ten psi (68.9 kPa) blast loading, the following conclusions are indicated:

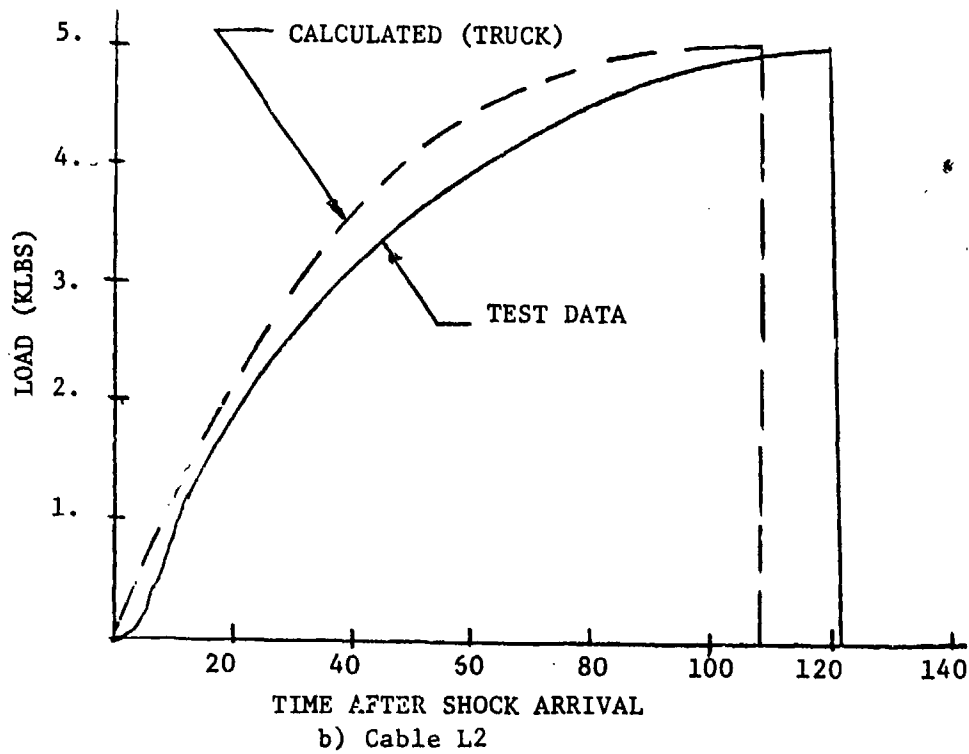
1. Finite element modeling techniques can be used to determine the strain response of shelter walls to blast loading. For the analysis of this report, an equivalent layer model of the wall was used, and the response was determined using the ADINA code.
2. The overturning behavior of a shelter due to blast loading effects can be predicted using the TRUCK computer code. Both shelter roll motions and guy cable load response were predicted using the code.
3. Test results demonstrated that a shelter can be hardened to withstand a nominal 10.0 psi incident shock loading using conventional shelter materials and construction techniques.

REFERENCES

1. Milligan, Roger W., Fanucci, Jerome P., Rodal, Jose J.A., and Lawrence J. Mente, "Research and Development of an ISC Rigid Wall Hardened Shelter," Kaman Avidyne Report KA TR-187, July 1981.
2. Zartarian, Garabed, Yeghiayan, Raffi P., and Lush, Allen M., "Preliminary Design of Hardened Tactical Shelters - Design Concepts and Test Planning," US Army Research and Development Command, ARBRL-CR-004-64, August 1981.
3. Bathe, Klaus - Jurgen, "ADINA - A Finite Element Program for Automatic Dynamic Incremental Nonlinear Analysis," M.I.T. Report 82448-1, September 1975 (Revised December 1978).
4. Lush, Allen, "Large Deflection Analysis of Sandwich Panels Using an Equivalent Layer" (unpublished manuscript), Presented at the 3rd ADINA Conference, M.I.T., 10 June 1981.



TIME AFTER SHOCK ARRIVAL (MSC)
a) Cable L1



b) Cable L2

Figure 12. Guy Cable Response to Shelter Overturning

5. Lee, William N. and Garabed Zartarian, "BLOCK - A Digital Computer Program for Calculating the Blast Loadings on Box-Like Structures," Kaman Avidyne Report TR-156, January 1979.
6. Crenshaw, William L., Milligan, Roger, W., and Jerome P. Fanucci, "Test and Evaluation of a Hardened ISO Shelter at MILL RACE," Presented at the MILL RACE Symposium, Harry Diamond Laboratories, March 1982.
7. Norris, Charles H., et al., Structural Design for Dynamic Loads, McGraw - Hill Book Company, Inc. New York, 1959.
8. Uhlenbeck, George, "Diffraction of Shock Waves Around Various Obstacles," Engineering Research Institute Report for ONR Project M720-4, University of Michigan, Ann Arbor, March 21, 1950.
9. Peery, David, J., Aircraft Structures, McGraw - Hill Book Company, Inc., 1950.
10. Lee, William N. and Norman P. Hobbs, "Truck 3.0 - An Improved Digital Computer Program for Calculating the Response of Army Vehicles to Blast Waves," Kaman Avidyne Report KA TR-171, September 1979.